Simulation of Missiles with Grid Fins using an Unstructured Navier-Stokes solver coupled to a Semi-Empirical Actuator Disc

Ph.Reynier[1] E. Schülein[2] & J.M. Longo[1]

1 Institut für Aerodynamik und Strömungstechnik, DLR, Lilienthalplatz 7,
38108 Braunschweig, Germany, corresponding author, Philippe.Reynier@dlr.de
2 Institut für Aerodynamik und Strömungstechnik, DLR, Bunsenstraße 10,
37073 Göttingen, Germany, Erich.Schuelein@dlr.de

Abstract

An actuator disc for grid fin simulations has been integrated in an unstructured code. This method consists in replacing the physical grid fins by artificial boundary conditions in the flow. The forces involved by the grid fins are computed using a procedure based on the semi empirical theory for lattice wings. The final tool is applied to the predictions of force and moment coefficients around a missile with grid fins which are compared to experimental data obtained for the same configuration. In addition, computations for a body alone have been performed to be used as reference. The results for a Mach number range from 1.8 to 4 show the capability of the method to predict the differences between the drags of the vehicle and the body. The numerical simulations with angle of attack show a good agreement with the experiments for the force coeficients and the pitching moment. This work shows the capabilities of the tool at different Mach numbers and angles of attack and its usefulness for the design of vehicles equipped with grid fins.

Introduction

Since the middle of the eighties, the lattice wings also called grid fins or lattice controls have been the object of a strong interest in the scientific community working on missile technology. In 1998, several papers presented at the *Applied Vehicle Technology Panel Symposium* held in Sorrento (Italy) were focusing on this topic [1, 2, 3, 4]. Different studies on lattice wings were dedicated to experimental investigations [5, 6], others to theoretical analysis [7, 8]) or to numerical studies of missile with lattice wings [9, 10]. The aerodynamic qualities of grid fins are known for a long time. They are very effective control devices and sometimes have advantages over monoplane wings [4]. Their performances in the supersonic regime and their relatively small

size make them very attractive for missile applications. They present two main inconvenients, they suffer a loss of stability in the transonic regime and have relatively high drag levels. The first inconvenient [3] is due to the fact that the grid fin cells choke in the transonic regime. The second has been the main concern which has during a long time restricted the use of this technique. However, in the last years some experimental studies [11, 12] have shown that grid fin drag levels can be considerably reduced by altering the frame cross-section shape and the web thickness with only a minimal impact on lift and other aerodynamic properties.

Since the nineties, different research activities on grid fins have been conducted by the DLR [13, 14]. Several test campaigns have been led [13, 15] to investigate different geometries of lattice wings and missiles with grid fins. In parallel to these experiments, numerical simulations, based on the actuator disc concept, have been carried out [16] for predicting force and moment coefficients of a missile with lattice wings. Several numerical studies [9, 10, 17] have shown that Navier-Stokes computations of missiles with grid fins compare well with experimental data. However, these simulations are expensive due to the complexity of the geometry and 80 % of the mesh is located in the grid fin region [17].

In order to save some computational effort an actuator disc has been developed [18] to simulate flows around a vehicle with lattice wings. Using this approach the lattice wings are replaced by an actuator disc and therefore, by artificial boundary conditions inside the flow, where the forces involved by the grid fins are taken into account in the balance equations. Initially this method [18] was coupled to an experimental database providing the force coefficients at the lattice wing locations. Several simulations have been performed for an isolated grid fin and a complete vehicle [14, 16]. The comparisons with the experimental data [13] have demonstrated the capabilities of the method but also the strong dependence of the numerical result reliability on the database range of validity. The actuator disc for lattice wings is now integrated in the TAU [19] unstructured solver developed by DLR. The actuator disc has not been coupled with a database but with a numerical procedure based on a semi-empirical theory for lattice wing [7]. Using this procedure the forces at the lattice wing location are computed as functions of geometrical parameters and flow conditions using semi-empirical formulae. The different relations have been validated and adapted when necessary using experimental data [20]. The numerical tool has been successfully applied to the prediction of the force coefficients of an isolated grid fin [23]. Here the code is applied to the prediction of the aerodynamic performance in terms of force and moment coefficients of a complete vehicle. This will assess the capacity of the tool to be used for the design of vehicles equipped with grid fins.

Numerical tools

Flow solver

The code TAU [19], developed by DLR, has been used for the numerical simulations. It solves the three-dimensional Navier-Stokes equations using a finite volume approach and can handle structured, unstructured and hybrid meshes built with prisms, pyramids, tetrahedra and hexaedra. The integration in time is carried out using an explicit Runge-Kuttta scheme. The space discretization is done using the AUSM-DV solver and dissipation terms are added to damp high frequency oscillations. The final scheme is accurate to the second order in space.

Actuator disc

In order to reduce the computational cost of the simulations around a missile with grid fins, as represented in Figure 1, an actuator disc has been developed [18]. Using this technique the grid fin is replaced by artificial boundary conditions within the flow, here resumed as follows (more details are given in [14, 18]).

The actuator disc theory is based on the application of the conservation laws for mass, momentum and energy. Using this technique, the grid fin is replaced by two sets of boundary conditions. At the upstream side of the actuator disc the characteristic theory is applied. Therefore, all the variables are extrapolated for a supersonic flow, while one has to be imposed for a subsonic flow. Here, for a subsonic flow the density and velocity components are extrapolated from inside the domain and the mass-flux is chosen as the variable to be prescribed (see[18]). Its value at the downstream boundary of the actuator disc is imposed while pressure and energy are calculated supposing that the total enthalpy remains constant.

The characteristic theory is also used at the downstream side of the actuator disc. As a consequence, four flow properties have to be imposed if the flow is subsonic while the fifth is extrapolated from inside the flow-field. The pressure or the velocity can be chosen. Previous results [18] have shown that the extrapolation of the velocity leads, from a physical point of view, to more realistic pressure distributions. As a consequence this method has been retained. For a supersonic flow, all the variables have to be imposed. In this case, all the flow variables at the downstream boundary are calculated from their respective values at the upstream boundary of the actuator disc.

These boundary conditions have been extended for turbulent flows using Neumann boundary conditions at the actuator disc for the turbulent quantities. This is a very rough approximation which does not account for the impact of the lattice wing on the turbulence. Downstream of the actuator disc, the flow has been modified by the impact of the lattice wing, therefore the local aerodynamic forces involved by the presence of the grid fin have to be determined. These forces are computed using semi-empirical relations as functions of the local flow conditions and geometrical parameters. Then, they are accounted for in the flux balance at the downstream side of the actuator disc.

Semi-empirical module

Downstream of the actuator disc, the flow characteristics are changed due to the impact of the lattice wing. Depending on grid fin geometry and local flow conditions in terms of Mach number, angle of attack and yawing angle, this impact has to be determined. For the previous studies [14, 18] using the actuator disc for lattice wings, the force coefficients were interpolated from an experimental database obtained from wind-tunnel experiments [4, 13] performed for an isolated grid fin. The numerical simulations for a complete missile [14, 16] showed strong discrepancies with the experiments [13] for angles of attack higher than 10 degrees. These differences were due to the presence of a vortical flow developing along the missile and impacting on one lattice wing. The resulting local flow conditions were transonic and the database was only valid from Mach 1.8 to 4. This investigation put in evidence the strong dependence of the reliability of the numerical results on the database.

Here, in order to extend the applicability of the method, the actuator disc is coupled with a numerical module [20] mainly based on a semi-empirical theory for lattice wings. Using this theory [7] which is the result of long-time experimental and numerical investigations, the force coefficients of the grid fins are computed using semi-empirical relations. The experimental results obtained at DLR [13, 15, 21, 22], for basic lattice wing configurations and a wide range of Mach numbers and angles of attack, have been used to complete and modify this theory which can be briefly described as follows. More details can be found in [20] .

The calculation of the grid fin performances takes advantage of the fact, that at all Mach numbers, the angle of attack corresponding to the maximum lift is considerably higher than for a monoplane wing. The neighbouring lifting planes of the grid fin induces a more favourable alignment of the flow. This delays the separation to higher angles of attack and causes a smooth separation at supercritical angles. The presence of orthogonal planes avoids the cross flows and gives a good basis for using the linear theory. Each plane of a grid fin corresponds to a high aspect ratio wing. Another simplification of the theoretical model is the independence of the load capacity of a lattice wing (for given plane spacing and wing sizes) on the internal arrangement of the grid (framework or honeycomb). This hypothesis is valid for all wings with a large number of cells. Therefore, each cell of the wing is considered to be a square box shaped wing, and its internal flow has an aerodynamic behaviour which is completely independent from the rolling over the longitudinal axis of the wing. The main geometrical parameters of the lattice wing are the wing height h, the wing span b, the plane thickness c and the distances between the neighbouring vertical and horizontal surfaces t_y and t_z. Usually the distances between the surfaces in a lattice wing are chosen in such a way that $t_z = t_y = t$. These grid fin qualities simplify the calculation of the induced aerodynamic forces at subsonic ($Ma < M_{cr_1}$), transonic ($Ma_{cr_1} < Ma < Ma_{cr_2}$) and supersonic regimes (when $Ma > Ma_{cr_2}$) separated by the two critical Mach numbers Ma_{cr_1} and Ma_{cr_2}. A sufficiently exact prediction of the performance of these wings, at any angles of attack and yaw, is performed through a simplified formulation of the flow around the lattice wing for each regime. The aerodynamic forces induced by the lattice wings are calculated for each regime using flow conditions and geometrical parameters.

At subsonic speeds, the calculation model is based on the lifting line scheme. The lift of the lattice wing is computed in two steps. First, each individual plane of the grid fin is supposed to be under the same conditions that one of the corresponding polyplanes with infinite span at the same effective angle of attack. Then, the lift of the grid is approximately equal to the lift of the corresponding polyplane of infinite span. The angle of attack of the corresponding polyplane of infinite span is determined by taking into account the average downwash angle from the free vortices of the grid. Afterwards, the induced drag of the wing as well as the friction drag are calculated. An additional half-empirical correction of the aerodynamic coefficients is determined by considering the real lattice wing dimensions.

As example, the axial coefficient of a lattice wing in the subsonic flow without flow separation is the sum of the axial friction, c_{x_f}, and lift, c_{x_i}:

$$c_x = c_{x_f} + c_{x_i}, \tag{1}$$

where the contribution of the friction is calculated from the skin friction coefficient c_f. As example for a honeycomb wing:

$$c_{x_f} = 2c_f(1 + \frac{h(b+t)}{b(h+t)}), \tag{2}$$

where c_f is computed using the usual relations valid for laminar or turbulent flows. This modelling is valid until the first critical Mach number M_{cr_1} is reached in a grid cell.

The model for transonic flows is applied when the sonic speed is reached in the narrowest cross section of the wing. This corresponds to the critical Mach number M_{cr_1}. Inside the grid fin this regime is characterized by the formation of strong shock waves and local supersonic zones. This involves an increase of the axial force of the wing through an additional wave drag c_{x_w}. As a consequence the axial force coefficient has now three components:

$$c_x = c_{x_f} + c_{x_i} + c_{x_w}. \tag{3}$$

The axial wave force of the lattice wing is calculated using an empirical correlation depending on the wing geometry.

For the calculation of the normal force coefficient, using the analogy between the grid cell and the one dimensional channel flow, it is demonstrated that the variation of the normal force with the Mach number of the main flow ($Ma_{cr_1} < Ma < 1$) or the subsonic flow behind the head wave ($1 < Ma < Ma_{cr_2}$) is proportional to the variation of the dynamic pressure.

With the achievement of the supersonic regime in the incoming flow a normal head shock wave comes upstream of the wing. There is no change in the flow inside the grid cells since the flow behind this head wave is subsonic. In principle the wing should have the same aerodynamic behaviour accepting that the flow parameters behind this shock wave as the parameters of a certain imaginary undisturbed flow. The wing drag changes since the strong shock wave leads to additionally total pressure losses.

The supersonic regime begins when the second critical Mach number, Ma_{cr_2}, is reached. Then, the flow becomes supersonic in the complete flow field between the neighbouring planes. In the region where $Ma > Ma_{cr_2}$ the flow between two planes of the lattice wing at moderate incidence angles can be calculated with analytic equations. Considering the emerging interactions of expansion fans or shock waves in different combinations together or with solid walls the pressure distributions on the wing surface and the induced forces (without friction drag) can be determined. As a result of mutual interaction between planes the lift coefficient of the lattice wing in this region is reduced comparing to the value typical of isolated planes. The axial force coefficient can be calculated as:

$$c_x = c_{x_f} + c_{x_p}, \tag{4}$$

where c_{x_p} is provided by the integration of the surface pressure. The friction component c_{x_f} is calculated like at smaller Mach numbers. As example for a honeycomb wing with Equation (2). At higher Mach numbers the shock waves and the expansion waves do not impact on the neighbouring planes. The surface pressure distribution on each wall is independent and corresponds to this of an isolated plane, therefore the previously physical model remains valid.

Using the semi-empirical lattice wing theory, the aerodynamic forces induced by a grid fin are calculated as functions of the flow conditions (Mach number, angles of attack and yaw) and grid fin geometrical characteristics (height, chord, span, spacing and plane thickness). A module based on this theory has been coupled with the unstructured Navier-Stokes solver TAU. The final code has been already applied on an isolated grid fin [23]. This has demonstrated the capability of the tool to reproduce the trends of the force coefficient evolution with the Mach number and the angle of attack. Here the tool is applied to the simulation around a complete missile to determine the influence of the grid fins on the vehicle overall performances.

Application to a missile

Configuration

The missile with grid fins computed has been already experimentally investigated [13]. The geometry is represented in Figure 1. In the wind-tunnel tests the model is maintained by a support which is not taken into account for the computations. The length of the missile is 480 mm, its diameter 52 mm. The missile has a sharp nose, the length of the straight part is 350 mm, the lattice wings are located at 30 mm from the base and are maintained close to the body by four arms which are neglected in the numerical simulations. Due to the symmetry of the configuration only half of the missile has been computed. In order to assess the influence of the lattice wings on the numerical results, a body alone has been also computed. This body corresponds to the vehicle described above without grid fins.

The meshes used to simulate the missile and the body alone have been generated with the CENTAUR [24] grid generator. For both configurations (see Figure 2), the computational domains extend over a little more than half of the vehicle length in the transverse direction and $1/3$ of the vehicle length downstream of the base. For each geometry, a first grid has been created then adapted using the adaptation module of TAU. This process has been carried out until the achievement of the grid convergence. The final mesh for the complete vehicle is approximately 400000 tetrahedra and 560000 prisms. For the body alone the mesh is around 443000 tetrahedra and 487000 prisms. This shows that using the actuator disc concept the size of the mesh required for the complete vehicle is almost the same than for a body alone. This is far to be the case when the complete vehicle is computed without the actuator disc approach: the mesh is then at least five time larger than for a body alone.

Computed cases

The geometries described above have been computed at Mach numbers 1.8, 2, 3 and 4. The different cases with the corresponding Mach and Reynolds numbers and angles of attack are resumed in Table 1. Computations have been performed for laminar and turbulent flows. For the turbulence modelling two models have been tested, the Spalart-Allmaras one equation model and the two-equation $k-\omega$ model of Wilcox. For Mach 4, three cases at 5, 10 and 20 degrees angles of attack have been computed in order to check the reliability of the tool in presence of a vortical flow. The case 6 has been computed for the current configuration but also for the same missile with different grid fins.

The boundary conditions applied to the computational domain are the followings. The walls are isothermal, the plane $y = 0$ is the symmetry plane, the other boundaries are the far-field. For the complete vehicle, at the lattice wing locations the actuator disc conditions are applied. On the lattice wing sides a supersonic outflow is imposed.

Vehicle without angle of attack

The cases 1 to 7 of Table 1 correspond to the computations of the vehicle and the body alone without angle of attack. As the multigrid technique is available with TAU [19] two grid levels

have been used for the computations. The computations have been started using the coarse grid and finished with the fine grid in order to save some computational effort. The CFL numbers use for the simulations varied from 2 for a laminar flow without angle of attack to 0.5 for the turbulent predictions at 20 degrees angle of attack. Depending on the computed case, between 15000 and 30000 iterations were required to achieve the result convergence using the AUSM-DV numerical scheme integrated in TAU [19].

At first, the influence of the turbulence modelling has been checked for a body alone. In Figure 3, the experimental data and the numerical results obtained for the drag, C_d, are plotted. The simulations show a good agreement between the laminar prediction and the experimental data at Mach 1.8. The drag is overestimated by both turbulent calculations. The Wilcox $k-\omega$ model provides a value of the drag which is not so far, around 10%, from the experimental value. This is not the case of the calculation with the model of Spalart-Allmaras where the difference with the experiments is around 20%. For this reason this model has not been used anymore in the computations. At Mach 4 the experimental data is underestimated by the laminar prediction while the $k-\omega$ model provides a good agreement. As this work focuses more on high Mach numbers the Wilcox $k-\omega$ model has been selected for all the computations of both body alone and complete missile. The discrepancies observed between the experiments and the numerical simulations are small (no more than 10%) and may originate from two sources. First, the turbulence modelling since the turbulence might not be fully developed. Second, the fact that the wind-tunnel model support is not here taken into account.

The complete missile has been computed at Mach 1.8, 2, 3 and 4 with the Wilcox $k-\omega$ model. The Mach number distribution around the vehicle at Mach 4 is shown in Figure 4. In order to cancel the influence of the wind-tunnel model support, instead of comparing the experimental and the numerical values of the drag for the complete vehicle, in Figure 5 the differences between the drags of the complete vehicle and the body alone obtained experimentally and numerically are plotted. For all cases the simulations recover more than 90% of the grid fin effects. Here, there is another source of discrepancy. The semi empirical theory for lattice wings here used is adapted to fins with uniform cells. Due to the fact that some cells of the current grid fin differ in shape, its drag is underestimated. This was also the case for an isolated lattice wing [23].

Furthermore, from a design point of view the most important is the capability of the tool to predict the same trends as observed in the experiments. Figure 5 shows that the numerical results predict, like in the experiments, almost a drag reduction by a factor two when the Mach number increases from 1.8 to 4. This demonstrates the validity of the actuator disc to predict the force changes on a vehicle with grid fins for different Mach numbers and without angle of attack.

To assess the capabilities of the code for design analysis the same missile has been computed with different grid fins. The vehicle is still equipped with honeycomb grid fins as in Figure 1 but the new fins have thinner inner and outer frame thicknesses. The configuration has been computed for the case 6 of Table 1. The numerical value obtained for the drag is reported in Figure 5 with the values obtained for the body alone and the missile with the previous lattice wings which are thicker. The results show that using another geometry for the lattice wings the drag of the complete vehicle can be tailored by 23%. The convergence of the numerical results is obtained after some hundreds of iterations and without additional mesh generation effort. This demonstrates the usefulness of the tool for system analysis during the design loops of vehicle equipped with lattice wings.

Presence of an angle of attack

In order to assess the validity of the method in presence of angle of attack some computations have been done for 5, 10 and 20 degrees angle of attack. These calculations are reported in Table 1 under the numbers 8 to 10. Both, complete vehicle and body alone have been computed. The predictions for the body are used as reference for estimating the capabilities of the actuator disc. The values predicted for the axial and normal forces and the pitching moment and the corresponding experimental data are presented in Figures 6 and 7. The predictions of the axial and normal forces for both body alone and complete missile are in good agreement with the experimental data for all angles of attack. The differences between the predictions and the experimental data is not higher than 8 %. This demonstrates the efficiency of the numerical tool in recovering the forces for the complete vehicle even in presence of angle of attack. The results for the pitching moment are shown in Figure 7. They are in general good with a small discrepancy at 10 degrees between the computed value and the experimental data.

Conclusions

The objective of this work was to develop a tool for the design of missiles with lattice wings. In this objective, an actuator disc for lattice wings already tested with a structured code has been integrated in TAU. Instead of being coupled to an experimental database, the code has been coupled with a numerical module based on the semi-empirical theory for lattice wings providing the force coefficients as function of flow conditions and grid fin geometry. The complete tool has been firstly tested on an isolated lattice wing and then applied to a missile with lattice wings. Several computations have been performed for a wide range of Mach numbers and angles of attack. In parallel, a body alone has been computed to be used as reference case for the complete vehicle.

The numerical results demonstrate the validity of the actuator disc approach for design and analysis of hypersonic vehicles equipped with grid fins. The changes in force and moment coefficients experienced by the missile due to the presence of the grid fins, are qualitatively very well reproduced and are quantitatively within a bound of about 10 % compared to the experimental data.

The required computer time for a complete configuration on a workstation is less than 20 % more than the time required for a body alone. The extra time corresponds to the additional mesh involved by the presence of the lattice wings and by the actuator disc. This is worth noting that a simulation of such a configuration without actuator disc would require a computational effort between four and six times more than for a body alone. Another advantage of the actuator disc technique is that so far the grid fin configuration (number of wings, size and position) remains constant, no additional time for the grid generation is necessary to test different lattice-wing geometries. Moreover, the new flow solutions are almost obtained without computational effort. Comparing to a complete simulation without actuator disc, this means an additional time saving of the order of weeks to analyse the impact of lattice wing geometry on missile performance.

Acknowledgements

The present work has been performed in the framework of the DLR HaFK project. The financial support of

the German Ministry of Defence and the project monitoring by Dr. H. Ciezki are gratefully acknowledged.

References

[1] Khalid M., Sun Y. and Xu H. "Computation of flows past grid fin missiles", In RTO MP 5, Proceedings of RTO AVT Symposium on Missile Aerodynamics, 12.1-12.11, 11-14 May, Sorrento, Italy, 1998.

[2] Kretzschmar R.W. and Burkhalter J.E. "Aerodynamic Prediction Methodology for Grid Fins", In RTO MP 5, Proceedings of RTO AVT Symposium on Missile Aerodynamics, 11.1-11.11, 11-14 May, Sorrento, Italy, 1998.

[3] Simpson G.M. and Sadler A.J. "Aerodynamic Prediction Methodology for Grid Fins", In RTO MP 5, Proceedings of RTO AVT Symposium on Missile Aerodynamics, 9.1-9.11, 11-14 May, Sorrento, Italy, 1998.

[4] Washington W.D. and Miller M.S. "Experimental investigations of grid fin aerodynamics: a synopsis of nine wind tunnel and three flight tests", In RTO MP 5, Proceedings of RTO AVT Symposium on Missile Aerodynamics, 10.1-10.13, 11-14 May, Sorrento, Italy, 1998.

[5] Brooks R.A. and Burkhalter J.E., "Experimental and analytical analysis of grid fin configurations", Journal of Aircraft, vol 26(9), 885-887, 1989.

[6] Burkhalter J.E., Hartfield R.J. and Leleux T.M., "Nonlinear Aerodynamic Analysis of Grid Fin Configurations", Journal of Aircraft, vol 32(3), 547-554, 1995.

[7] Belotserkovsky S.M., Odnovol L.A., Safin Yu.Z., Tylenev A.I., Prolov V.P. and Shitov V.A., "Reshetchatye krylia", Maschinostroenie, 320 p., Moskow, 1985.

[8] Burkhalter J.E. and Frank H.M., "Grid fin aerodynamics for missile applications in subsonic flow", Journal of Spacecraft and Rockets, vol 33(1), 38-44, 1996.

[9] Lin H., Huang J-C. and Chieng C-C., "Navier-Stokes computations for body/cruciform gridfin configuration", AIAA Paper, 2002-2722, 20^{th} AIAA Applied Aerodynamics Conference, June 24-27, St. Louis, Mo, 2002.

[10] Sun Y. and Khalid M., "Prediction of supersonic flow around a grid fin missile using NPARC", In Proceedings of 5^{th} Annual Conference of the Computational Fluid Dynamics Society of Canada, CFD 97, May 25-27, Victoria, BC, Canada, 1997.

[11] Miller M.S. and Washington W.D., "An experimental investigation of grid fin drag reduction techniques", AIAA Paper, 94-1914-CP, June, 1994.

[12] Washington W.D. and Miller M.S., "An experimental investigation of grid fin drag reduction techniques", AIAA Paper, 93-0035, 31^{st} Aerospace Sciences Meeting & Exhibit, Jan. 11-14, Reno, NV, 1993.

[13] Esch H., "Aerodynamisches Beiwerte der Längsbewegung eines Flugkörpers mit Gitterleitwerk im Überschall", DLR Internal Bericht, IB 39113-2000C34, Köln, 2000.

[14] Reynier Ph. , Reisch U., Longo J. and Radespiel R., "Flow prediction around a missile with lattice wings using the actuator disc concept", to be published in Aerospace Science and Technology, 2003.

[15] Esch H., "Kraftmessungen an Gitterleitwerken im Überschall", DLR Internal Bericht, IB 39113-99C11, Köln, 1999.

[16] Reynier Ph., Reisch U., Longo J. and Radespiel R., "Numerical study of hypersonic missiles with lattice wings using an actuator disk", AIAA Paper, 2002-2719, 2002-2719, 20^{th} AIAA Applied Aerodynamics Conference, June 24-27, St. Louis, Mo, 1993.

[17] DeSpirito J., Edge H.L., Weinacht P., Sahu J. and Dinavahi P.G., "Computational fluid dynamics analysis of a missile with grid fins", Journal of Spacecraft and Rockets, vol 38(5), 711-718, 2001.

[18] Reisch U., "Simulation of lattice wings with the actuator disk concept", DLR Internal Bericht, IB 129-2000/13, Braunschweig, 2000

[19] Gerhold T., Friedrich O., Evans J. and Galle M., "Calculation of complex three dimensional configurations employing the DLR TAU code", AIAA Paper, 97-0167, 1997.

[20] Schülein E., "Expertensystem zur Auslegung und Optimierung isolierter Gitterflügeln", DLR Internal Bericht, in preparation, Göttingen, 2003.

[21] Esch H., "Kraftmessungen an einem Flugkörper mit Gitterleitwerken im Überschall", DLR Internal Bericht, IB 39113-97C11, Köln, 1997.

[22] Esch H., "Vortests zur Erweiterung des Datensatzes einer Flugkörperkonfiguration mit Gitterleitwerken", DLR Internal Bericht, IB 39113-2000C01, Köln, 2000.

[23] Reynier Ph. and Schülein E., "Incorporation of an actuator disc for lattice wings in an unstructured Navier-Stokes solver", Notes on Numerical Fluid Mechanics, Proceedings of the 13$^{\text{th}}$ DGLR/STAB Symposium, Munich, Germany, 12-14 Nov. 2002), Springer-Verlag, in press, 2003.

[24] Anon., "Online User's Manual", http://www.centaursoft.com/support/manual/.

Case	Mach number	Reynolds number	Angle of attack	Approach
1	1.8	1.8 10^6	0	Laminar
2	1.8	1.8 10^6	0	Wilcox
3	2	1.9 10^6	0	Wilcox
4	3	2.5 10^6	0	Wilcox
5	4	3.3 10^6	0	Laminar
6	4	3.3 10^6	0	Wilcox
7	4	3.3 10^6	0	Spalart-Allmaras
8	4	3.3 10^6	5	Wilcox
9	4	3.3 10^6	10	Wilcox
10	4	3.3 10^6	20	Wilcox

Table 1: Mach and Reynolds numbers, angles of attack and boundary layer modelling of the different computed cases for the complete vehicle and the body alone. The turbulence models are the two-equation $k-\omega$ model of Wilcox and the one-equation model of Spalart-Allmaras.

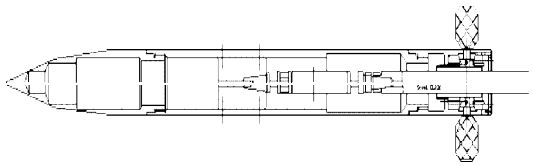

Figure 1: Missile with lattice wings experimentally investigated by Esch [13]. In the picture, the wings are parallel to the body for visualisation purposes.

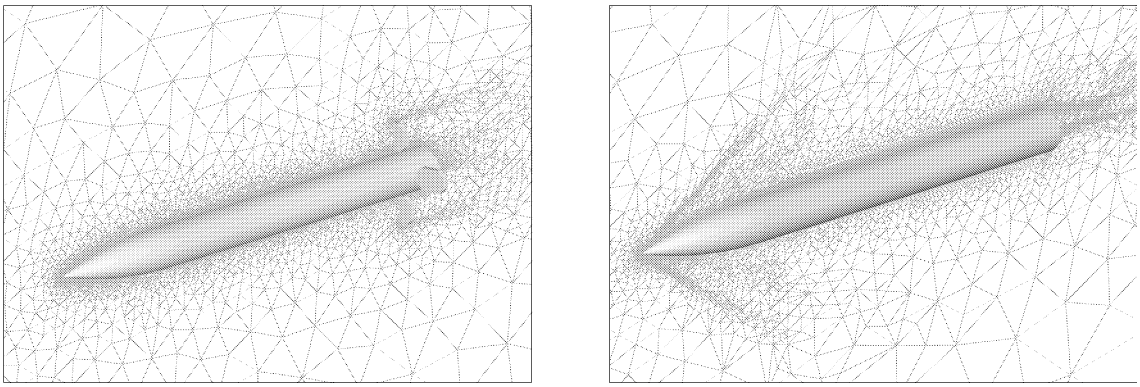

Figure 2: Symmetry planes of the hybrid meshes used to compute the complete vehicle (on the left side) and the body alone (on the right side).

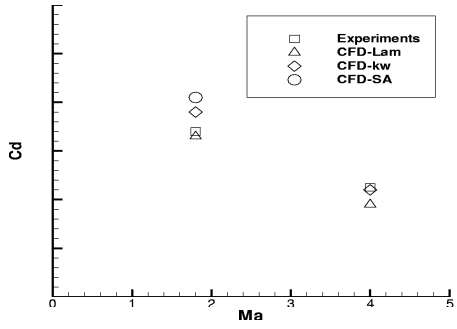

Figure 3: Experimental data and numerical values of the drag for the body alone at Mach 1.8 and 4. Lam is the laminar result, kw corresponds to the Wilcox $k-\omega$ model and SA to the model of Spalart-Allmaras.

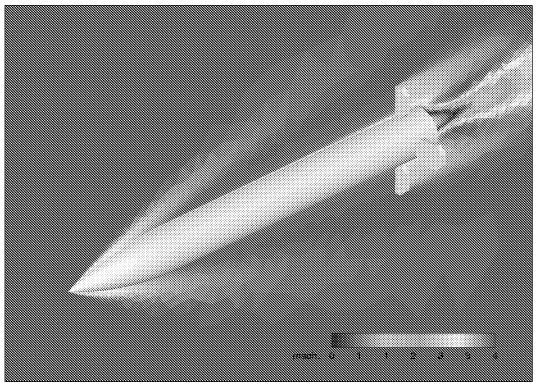

Figure 4: Mach number distribution around the complete missile at Mach 4 without angle of attack and with the $k-\omega$ Wilcox turbulence mode.

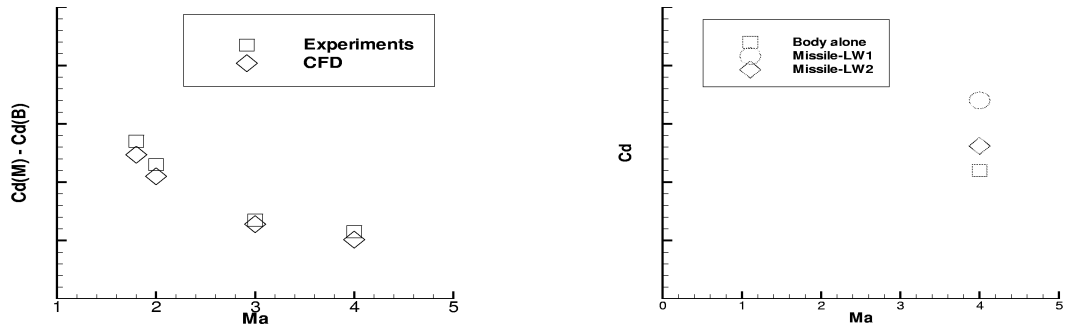

Figure 5: On the left: Differences between the drags of the complete missile (Cd(M)) and the body (Cd(B)) obtained numerically and experimentally. On the right: Drags of the body, the complete missile (Missile-LW1) and the missile with thinner grid fins (Missile-LW2) at Mach 4.

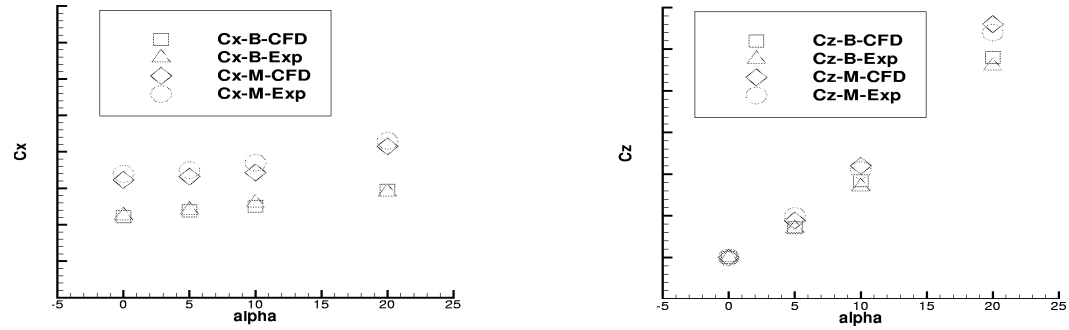

Figure 6: Experimental and numerical axial (on the left) and normal (on the rignt) force coefficients as functions of the angle of attack. Cx-B-Exp, Cx-B-CFD, Cz-B-Exp, Cz-B-CFD are for the body alone and Cx-M-Exp, Cx-m-CFD, Cz-M-Exp, Cz-m-CFD for the complete vehicle.

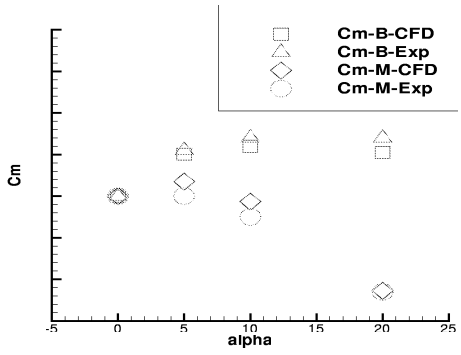

Figure 7: Experimental and numerical pitching moment coefficients for the body alone (Cm-B-Exp and Cm-B-CFD) and the complete vehicle (Cm-M-Exp and Cm-M-CFD) as function of the angle of attack.